THE PUBLISHING HOUSE
OF THE ROMANIAN ACADEMY

PROCEEDINGS OF THE ROMANIAN ACADEMY, Series A,
Volume 15, Number 2/2014, pp. 182–190

IMPROVING DRAFT TUBE HYDRODYNAMICS OVER A WIDE OPERATING RANGE

Tiberiu CIOCAN[1], Romeo SUSAN-RESIGA[1], Sebastian MUNTEAN[2]

[1] Hydraulic Machinery Department, "Politehnica" University of Timişoara
[2] Center for Fundamental and Advanced Technical Research, Romanian Academy – Timişoara Branch
Corresponding author: Romeo SUSAN-RESIGA, Bd. Mihai Viteazul 1, RO-300222, Timişoara,
E-mail: resiga@mh.mec.upt.ro

The paper presents a methodology for reducing the hydraulic losses in the draft tube of hydraulic turbines within a wide operating range, from part-load to full-load. The velocity field at the draft tube inlet is parameterized by taking into account the runner blade geometry at the trailing edge via the so-called swirl-free velocity. It is shown that by changing this swirl-free velocity profile one can significantly reduce the weighted-average hydraulic losses while improving the performances of the draft tube.

Key words: draft tube, swirl-free velocity, hydraulic losses, pressure recovery

1. INTRODUCTION

Over the last few decades, a greater demand in turbomachinery performances can be clearly perceived. Today, a higher efficiency is commonly expected for hydraulic turbines. Under such conditions, the improvements are coming from small details leading to competitive products based on new control techniques [1]. Moreover, a lot of the hydraulic turbines have to be refurbished in the next period [2]. Therefore, new demands on the deregulated energy market make it attractive to improve energetic, cavitational and dynamic performances of the hydraulic turbines over a wide operating range. However, the refurbishment procedure involves a new runner and maybe new guide vane blades while the rest of the hydraulic turbines components remain unchanged. An important component of a medium and low head reaction turbine is the draft tube. Since the draft tube losses have an important impact on the overall turbine performances. Vu and Retieb [3] clearly showed that the hydraulic losses in the draft tube are dominant at off-design conditions. Galvan [4] noticed that it is still a challenge to get the optimal flow distribution at the draft tube inlet which gives the best machine performance over a range of operating points.

Therefore, it is essential to develop a suitable parameterization of the swirling flow downstream the turbine runner in order to be analyzed the draft tube response to various inflow configurations [5]. Susan-Resiga et al. [6] have developed a new mathematical model for describing the swirling flow at the draft tube inlet of a Francis turbine within operating range, prior to the runner design. This model introduces the swirl-free velocity concept in order to parameterize and control the swirling flow kinematics at the runner outlet. As it is shown in [7], the swirl-free velocity profile supports a simple linear parameterization $v_{sf} = v_{sf}^{ave} + v_{sf}^{slo}(y - y_w/2)$, where $y \equiv r^2$ is the auxiliary radial coordinate, y_w the value at the cone wall. The average v_{sf}^{ave} and the slope v_{sf}^{slo} of the swirl-free velocity profile are considered the optimization parameters, respectively. Further, in this theory, the dimensionless discharge q and the dimensionless flux of moment of momentum m are the two integral quantities that characterized the swirling flow at variable regimes. The distributions $m_1(q)$ (blue line) upstream and $m_2(q)$ (red line) downstream to the GAMM Francis runner are plotted in Fig. 1. The dimensionless flux of moment of momentum $m_1(q)$ generated by the guide vane blades is ingested by the runner while $m_2(q)$ is the residual value leaved downstream to the runner then ingested by the draft tube. In our case, six operating points (black filled squares) were arbitrary chosen

between $q = 0.26...0.36$ in the procedure (Table 1). Each operating point is characterized by a pair (q, m_2). In the last column of the Table 1 is associated a weight for each operating point in order to be computed the weighted averaged losses of the draft tube.

Table 1

Investigated operating points at constant energy

Operating points	Dimensionless discharge Q	Dimensionless flux of moment of momentum m_2	Weight w
OP1	0.26	0.256064E-01	10%
OP2	0.28	0.229478E-01	20%
OP3	0.30	0.191041E-01	20%
OP4	0.32	0.139218E-01	20%
OP5	0.34	0.721656E-02	20%
OP6	0.36	-0.123287E-02	10%

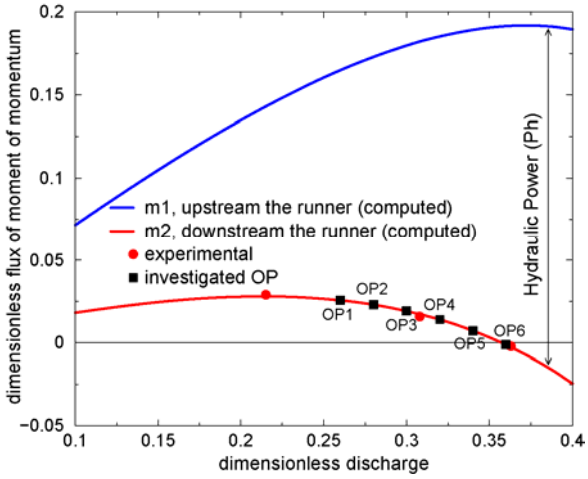

Fig. 1 – Dimensionless flux of moment of momentum versus the dimensionless discharge at constant energy for GAMM Francis turbine model.

The paper presents a methodology for improvement the draft tube performances taking into account the minimum losses. Therefore, the velocity profiles at the draft tube inlet are generated using a mathematical model a-priori to the runner design. Section 2 details the problem set-up, the boundary conditions and the computational domain considered in our case. The optimization procedure and the objective function are shown in Section 3. The parametric representation of the swirl-free velocity profile is described being the subject of optimization in order to achieve the minimum hydraulic losses of the draft tube on the extended range. In Section 4, the flow analysis is presented and the improvements are outlined. The conclusions are drawn in the last section.

2. PROBLEM SET-UP

The draft tube geometry and the structured mesh used in problem is shown in Fig. 3a while the distribution of the dimensionless cross-section area $A/A_{inlet} = A/\left(\pi R_{inlet}^2\right)$ versus the dimensionless curvilinear coordinate with respect to the radius R_{inlet} is plotted in Fig. 3b. One can observe that the draft tube length is approximately one order of magnitude larger than the radius of the inlet section whilst the area of the draft tube outlet is roughly four times larger than the area of the inlet section.

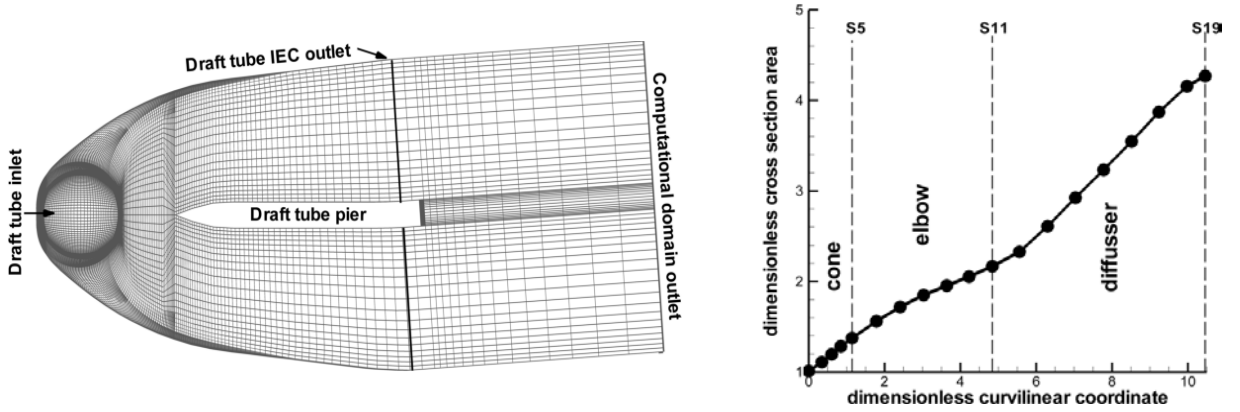

Fig. 3 – 3D computational domain and spatial discretization (a) and dimensionless cross section area distribution *versus* dimensionless curvilinear coordinate along to the draft tube (b).

The draft tube includes one pier being asymmetric with respect to a turbine meridian plane (i.e. a plane containing the turbine axis). This geometry is different than the original draft tube of the GAMM Francis turbine [8]. The asymmetric draft tubes with length around five inlet diameters (ten inlet radius) was found to have improved performances by Gubin et al. [9].

The computational domain is extended further downstream from the actual draft tube IEC outlet section [10]. The inlet section of the draft tube has the radius R_{inlet} = 0.201 m, while the reference radius is R_{ref} = 0.2 m, leading to a dimensionless inlet radius $r_{w\ inlet}$ = 1.005. A structured mesh with 501360 cells was generated using Gambit [11]. The velocity components and turbulent quantities are prescribed on the inlet section of the draft tube while the static pressure is imposed on the outlet section [5]. The radial profiles of the velocity components are computed using the mathematical model developed by Susan-Resiga et al. [6]. The three-dimensional flow is computed using FLUENT software [12] considering water as working fluid.

3. OPTIMIZATION PROCEDURE

The optimization process goal is to determine the global extreme value (minimum or maximum) of a function $f(x)$ denoted *objective function*. The objective function depends on several variables $f = f(x_1,...,x_n)$ called *control variables*. In our case, the control variables are considered both parameters of the swirl-free velocity profile (average v_{sf}^{ave} and slope v_{sf}^{slo}, respectively). The weighted relative head loss of the draft tube *DTLOSS* is a weighted average value of the relative head loss h_{rDT} defined according to the eq. (1) being considered the objective function in the optimization process. As a result, it is the main criterion in order to find the optimum swirl-free velocity configuration.

$$\mathrm{DTLOSS} = \sum_{OP=1}^{6} w_i \left(h_{rDT}\right)_i [-], \tag{1}$$

where w is the weight associated to each operating point from Table 1 and h_{rDT} the relative dimensionless head loss of the draft tube is computed using eq. (2). Particularly, the dimensionless head $h = 1.07$ of GAMM turbine is considered. It is more intuitive to express the draft tube head loss as percent of the turbine head,

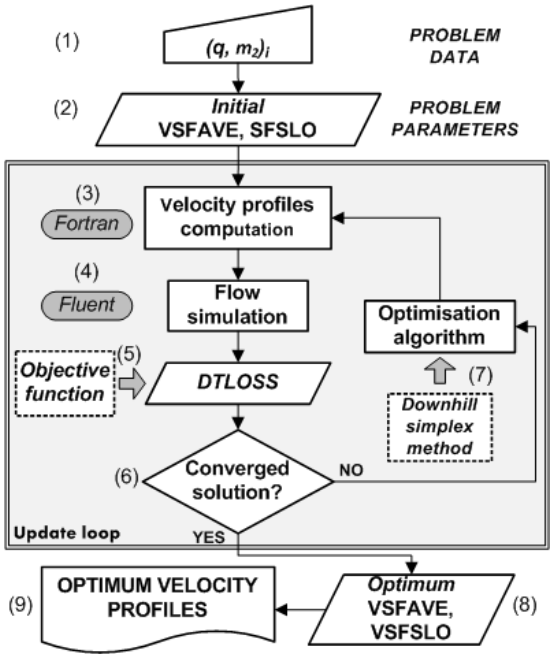

Fig. 4 – Draft tube inlet velocity profile optimization flow chart/

$$h_{rDT} = \frac{h_{DT}}{h} \times 100 = \\ = \frac{\text{draft tube head loss (energy loss)}}{\text{turbine head (energy coefficient)}} \times 100 \quad [\%], \tag{2}$$

where the dimensionless draft tube loss h_{DT} is defined in next equation:

$$h_{DT} = f/q \tag{3}$$

and the dimensionless hydraulic power loss f is computed as follows:

$$f = F^{IEC} \Big/ \left(\frac{\pi}{2} \rho \omega^3 R_{ref}^5 \right). \tag{4}$$

The hydraulic power loss F^{IEC} from eq. (4) is computed as a difference between the flux of total pressure from the draft tube inlet and the outlet sections according to IEC 60193 [10]. The flux of total pressure on the outlet section is computed using the average wall static pressure $p_{out:wall}$ and the average discharge velocity (Q/A_{out}) in following equation:

$$F^{IEC} = \int_{S_{in}} \left(p + \frac{\rho V^2}{2} \right) \mathrm{d}S - Q \left[p_{outwall} + \frac{\rho}{2} \left(\frac{Q}{A_{out}} \right)^2 \right] [W]. \tag{5}$$

Note that F^{IEC} defined in eq. (5) includes the excess losses of the kinetic energy at the draft tube outlet due to the large flow non-uniformity.

Downhill Simplex Method (DSM) [13, 14] is used in order to found the minimum value of the objective function *DTLOSS*. The optimisation procedure is shown in Fig. 4 with following steps: (1) the data pairs (q, m_2) corresponding to the six investigated operating regimes are selected; (2) the first guess of both initial parameters $v_{sf}^{ave} = 0.328$ and $v_{sf}^{slo} = 0$ corresponding to the trailing edge of the Francis runner blade geometry designed using a classical methodology [15]; (3) the velo-city profiles at the draft tube inlet for each operating point are computed based on the mathematical model for constrained swirling flow [6] implemented in FORTRAN using the International Mathematics and Statistics Library (IMSL) numerical library [16]. As a result, the velocity profiles are written in files (with *prof* extension) in order to be ingested by FLUENT expert code; (4) the steady three-dimensional turbulent flow is computed using realizable k-ε turbulence model for each operating point (six operating points are computed for each pair of problem parameters) with the inflow conditions determined at previous step; (5) the objective function DTLOSS is computed according to eq. (1) with associated weights from Table 1; (6) the solution is checked and the stopping decision in triggered when the objective function reaches the global minimum value, meaning the optimisation algorithm converged to a solution. As a result, the optimized configuration of the control variables is obtained (8), leading to the improved velocity profile at the draft tube inlet (9) plotted in Fig. 5. Otherwise, the process will continue by adjusting the control variables through the optimisation algorithm (7) until the objective function will not improve for any possible configuration of the control variables. The improved configuration of the swirl-free velocity profile associated to the actual draft tube corresponds to $v_{sf}^{ave} = 0.32$ and $v_{sf}^{slo} = 0.125$ leading to the minimum weighted relative head loss of the draft tube DTLOSS = 1.857 %. The initial and improved values of the problem parameters as well as the associated value of DTLOSS can be found in Table 2. The draft tube inlet velocity profiles corresponding to initial and improved configurations are shown in Fig. 5.

One can see in Fig. 5a that the initial swirl-free velocity configuration corresponds to a jet axial velocity profile near the axis for all operating points except OP1. The jet axial velocity profile presents a velocity excess near the axis. On the other hand, a significant deceleration of the axial velocity near the axis is observed for the improved swirl-free velocity configuration (Fig. 5b). Consequently, the velocity profiles associated to the operating points (OP1 and OP2) show a deficit near to the axis. Therefore, these profiles are called wake velocity profiles. In both cases the circumferential velocity is either co-rotating or counter-

rotating with respect to the runner direction, [17]. As the discharge increases, the axial velocity reaches a quasi-constant distribution, while the circumferential velocity goes from co-rotation with respect to the runner, at part load, to counter-rotation at full load [5]. However, an increased circumferential velocity component is distinguished near the wall at improved configuration with respect to the initial one.

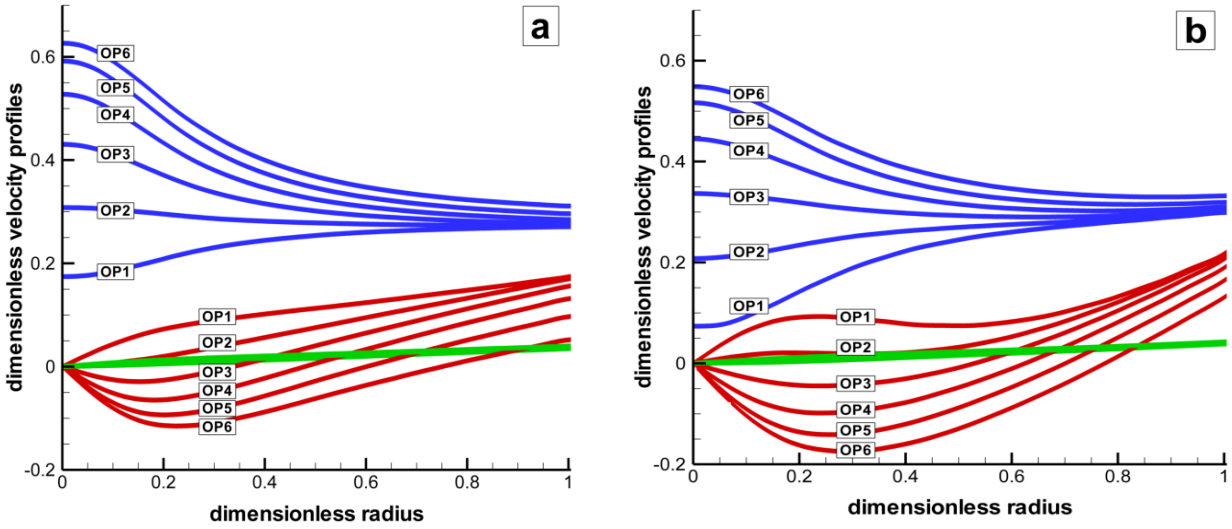

Fig. 5 – Velocity components profiles at the draft tube inlet: axial (blue), circumferential (red), radial (green): a) the swirl-free velocity configuration corresponding to the initial runner; b) the swirl-free velocity configuration corresponding to the improved runner.

4. ANALYSIS OF THE DRAFT TUBE HYDRODYNAMICS

Several cross-sections are defined in the draft tube in order to be analyzed the flow deceleration from the inlet to the outlet, Fig. 6. These planar cross-sections are built normal to the curvilinear line which connects the center points of all sections (orange points and line in Fig. 6). The analysis is focussed on the evolution

Table 2

Swirl-free velocity configurations

Swirl-free velocity	v_{sf}^{ave}	v_{sf}^{slo}	*DTLOSS* [%]
Initial configuration	0.328	0.000	2.308
Improved configuration	0.32	0.125	1.857

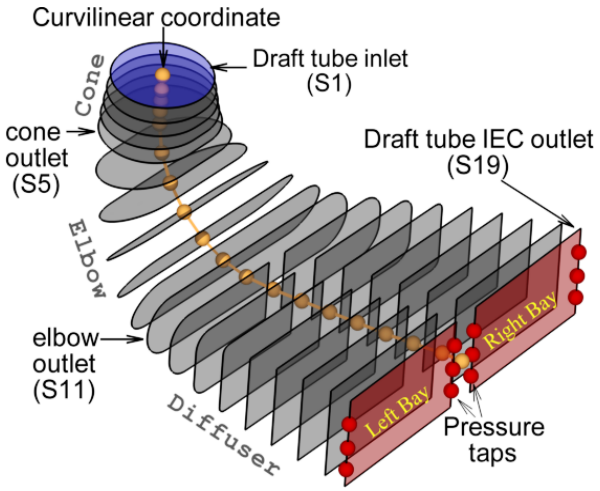

Fig. 6 – 3D computational domain and draft tube cross-sections.

of the kinetic energy fluxes along to the draft tube in order to capture the distribution of the flow non-uniformity which is directly linked with hydraulic losses. Consequently, the following integral quantities are defined in order to allow us to perform a detailed analysis of the draft tube hydrodynamics:

$$F_{kin} = \int_S \rho \frac{V^2}{2} \vec{V} \cdot \vec{n} \, dS \quad [W] \tag{5}$$

$$F_{kin}^{(n)} = \int_S \rho \frac{V_n^2}{2} \vec{V} \cdot \vec{n} \, dS \quad [W] \tag{6}$$

$$F_{kin}^{(t)} = \int_S \rho \frac{V_t^2}{2} \vec{V} \cdot \vec{n} \, dS \quad [W] \tag{7}$$

$$F_{kin}^{(ideal)} = Q \frac{\rho}{2} \left(\frac{Q}{S} \right)^2 \quad [W], \tag{8}$$

where $V_n = \vec{V} \cdot \vec{n}$ is the normal velocity component on the cross-section and V_t the tangential velocity component within the cross-section. The next relation is written $V^2 = V_n^2 + V_t^2$.

Firstly, the flux of kinetic energy F_{kin} is computed according to eq. (5). Secondly, the normal $F_{kin}^{(n)}$, eq. (6) and the tangential $F_{kin}^{(t)}$, eq. (7) components of the flux of kinetic energy are defined in order to discriminate between two components. However, the tangential component of the flux of kinetic energy $F_{kin}^{(t)}$ is easier to be computed using eq. (9). On the other hand, the ideal flux of kinetic energy, $F_{kin}^{(ideal)}$ eq. (8) corresponds to a flow with constant average discharge velocity on each cross-section. This is associated to the uniform flow with minimum kinetic energy. It will be taken as reference value further in our analysis. Therefore, the excess of kinetic energy $F_{kin}^{(excess)}$ is defined as the difference between the flux of kinetic energy F_{kin} and ideal one $F_{kin}^{(ideal)}$, eq. (10). Always the flux of kinetic energy will be larger than ideal one due to the flow non-uniformity. The flow non-uniformity is quantified with the coefficient ζ, eq. (11).

$$F_{kin}^{(t)} = F_{kin} - F_{kin}^{(n)} \quad [W] \tag{9}$$

$$F_{kin}^{(exces)} = F_{kin} - F_{kin}^{(ideal)} \quad [W] \tag{10}$$

$$\xi = F_{kin} / F_{kin}^{(ideal)} \quad [-]. \tag{11}$$

Conclusively, the relationship between the actual kinetic energy flux F_{kin} through a cross-section and it ideal value $F_{kin}^{(ideal)}$ can obviously be expressed either as a difference, eq. (10) or as a ratio, eq. (11). Both versions are relevant for the complex analysis of the draft tube hydrodynamic quantifying the deviation from uniform flow (with minimum losses).

The comparison between initial and improved hydrodynamic fields was performed for all investigated operating point. In this paper, only the numerical results for OP3 are plotted in Fig. 7. The flux of specific kinetic energy along to the draft tube corresponding to the initial and the improved swirl-free velocity profiles, respectively.

It can be seen that almost half of the kinetic energy is recovered in the cone and about only one quarter remains at the elbow outlet for both swirl-free velocity configurations associated to the initial and improved runners. The difference occur in the last part of the draft tube called diffuser (see Fig. 6) where for the initial swirl-free velocity configuration corresponding to the initial runner, the flux of specific kinetic energy F_{Kin} is quasi-constant compared with the ideal flux of kinetic energy $F_{kin}^{(ideal)}$. This means that the kinetic energy is no longer recovered in the draft tube diffuser being well quantified through the excess of kinetic energy $F_{kin}^{(excess)}$ up to the draft tube outlet. On the other hand, the differences between F_{kin} and $F_{kin}^{(ideal)}$ is small from inlet to outlet, thus resulting in a very small excess of kinetic energy at the draft tube outlet for the improved swirl-free velocity configuration. Practically, the tangential component of the kinetic energy flux $F_{kin}^{(t)}$ is recovered in the first two parts of the draft tube named cone and elbow.

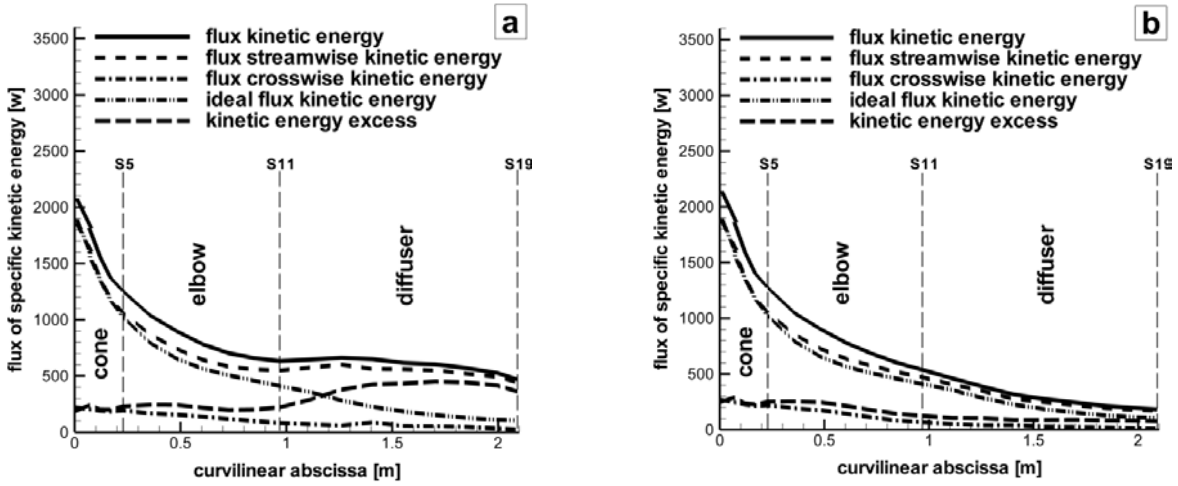

Fig. 7 – The flux of specific kinetic energy distribution along to the draft tube at **OP3**: initial (**a**) and improved (**b**) swirl-free velocity configurations.

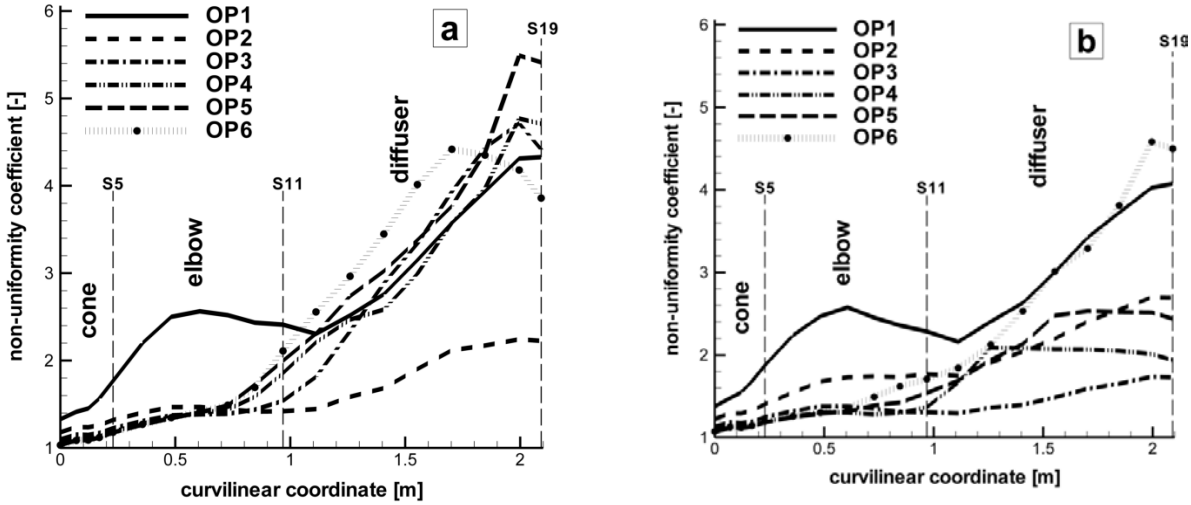

Fig. 8 – The distribution of the flow non-uniformity along to the draft tube for all operating points: initial (**a**) and improved (**b**) swirl-free velocity configurations.

The flow non-uniformity in the draft tube is quantified by ζ coefficient, eq. (11). The distribution of the flow non-uniformity along to the draft tube is plotted in Fig. 8 for all investigated operating points. One can observe a significant improvement between the distributions of the flow non-uniformity along to the draft tube with improved swirl-free configuration Fig. 8b with respect to the initial configuration Fig. 8a. The previous statement is supported by DTLOSS improvement with approximately 20% with respect to the initial configuration, respectively. The minimum value of the flow non-uniformity between the inlet and the outlet sections of the draft tube corresponds to OP2 at initial configuration with respect to OP3 at improved configuration. That means the operating point associated with minimum flow non-uniformity is shifted to larger discharge for improved configuration with respect to initial one.

Particularly, the distribution of the flow non-uniformity along to the draft tube corresponding to the operating point with the lowest discharge OP1 is completely different than other operating points. The distribution of the flow non-uniformity along to the draft tube at OP1 is the same for both configurations.

The flow non-uniformity is relatively small in the cone and the elbow for both swirl-free velocity configurations. The differences between the initial configuration and the improved one occur in the draft tube diffuser. The flow non-uniformity increases in the diffuser if a fraction of the cross-section is occupied by the main flow and a large dead-water region is developed in the rest of the cross-section [18]. The flow non-uniformity is lower in the diffuser at the improved swirl-free velocity configuration, Fig. 8b, excepting the operating points from the extremities (with the lowest and the largest values of discharge).

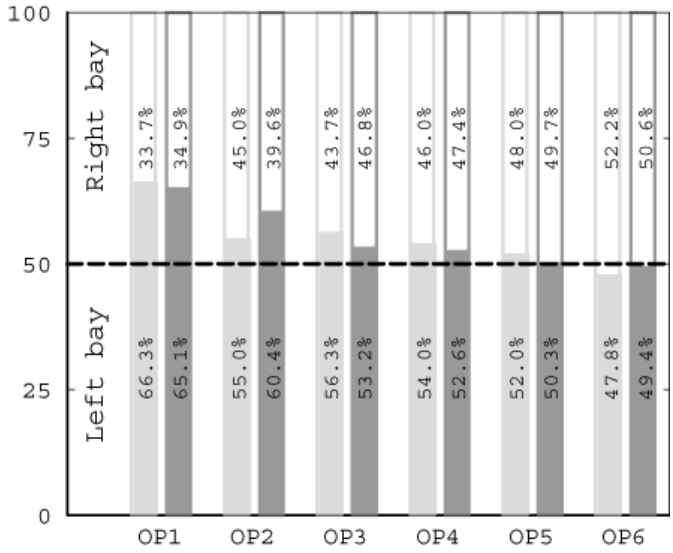

Fig. 9 – Discharge repartition in draft tube bays for initial (light grey) and improved (dark grey) configurations.

The discharge is not evenly distributed among the draft tube bays, Fig. 9. It can be seen that at OP1, the discharge in the left bay is practically half the discharge through the right channel in both configuration cases. The swirl direction changes from co-rotating to counter-rotating with respect to the runner as the turbine discharge is increased. As a result, the discharge in the left bay becomes larger than the discharge in the right bay at OP6. Overall, for the improved case, excepting OP2, the discharge repartition is closer to the ideal distribution (50% left bay – 50% right bay). Equalization of the flow in the draft tube bays is one of the untapped reserves for increasing the efficiency of the hydraulic turbine [9].

5. CONCLUSIONS

We present a complete methodology to improve the performances of a draft tube while the hydraulic turbine is operated within a range of discharge values including part-load and full-load regimes. The velocity field is determined prior knowing the runner, and a simple two-parameter representation is used, related to the runner outlet geometry via the swirl-free velocity profile. The objective function corresponds to the weighted averaged relative head loss in the draft tube DTLOSS, which is minimized for the improved swirl-free velocity configuration. Downhill Simplex Method is used in order to find the minimum value of the objective function DTLOSS. This procedure is applied for a Francis turbine with medium specific speed. As a result, the objective function DTLOSS is improved by approximately 20% with respect to the initial configuration. The improved swirl-free velocity profile is characterized by following parameters $v_{sf}^{ave} = 0.32$ and $v_{sf}^{slo} = 0.125$. The improved velocity profiles at the draft tube inlet are characterized by a significant deceleration of the axial velocity near the axis and larger values near the draft tube cone wall with respect to the initial velocity profiles. The coefficient ζ is introduced in order to quantify the flow non-uniformity along to the draft tube. The flow non-uniformity is relatively small in the cone and the elbow for both swirl-free velocity configurations. The differences between the existing configuration and the improved one occur in the draft tube diffuser. The minimum value of the flow non-uniformity between the inlet and the outlet sections of the draft tube corresponds to OP2 at initial configuration with respect to OP3 at improved configuration. That means the operating point associated with minimum flow non-uniformity is shifted to larger discharge for improved configuration with respect to initial one. Once the improved configuration of the swirling flow ingested by the draft tube is determined, the following task would be to design a runner delivering such a flow field using modern approach based on fully three-dimensional inverse design methods for turbomachinery blades [19].

ACKNOWLEDGEMENTS

Mr. Ciocan T. was partially supported by the strategic grant POSDRU 107/1.5/S/77265 (2010) of the Ministry of Labour, Family and Social Protection, Romania, co-financed by the European Social Fund – Investing in People. Prof. Susan-Resiga R. and Dr. Muntean S. were supported by the Romanian Academy program "Swirling flow analysis and instabilities control in turbomachinery".

REFERENCES

1. BOSIOC, A.I., TĂNASĂ, C., MUNTEAN, S., SUSAN-RESIGA, R., *Pressure recovery improvement in a connical diffuser with swirling flow using water jet injection,* Proc. of the Romanian Academy, Series A, **11**, *3*, pp. 245–252, 2010.
2. GOLDBERG, J., LIER, O.E., *Rehabilitation of Hydropower: An introduction to Economic and Technical Issues*, World Bank, Washington, D.C., 2011.
3. VU, T.C., RETIEB, S., *Accuracy assessment of current CFD tools to predict hydraulic turbine efficiency hill chart*, Proc. of the 21st IAHR Symposium on Hydraulic Machinery and Systems, Vol. 1, École Polytechnique Fédérale de Lausanne, Lausanne, Switzerland, 2002, pp. 193–198.
4. GALVAN, S.R., *Optimization of the inlet velocity profile of the Turbine99 draft tube*, PhD Thesis, École Polytechnique de Montréal, Canada, 2007.
5. SUSAN-RESIGA, R.F., MUNTEAN, S., CIOCAN, T., JOUBARNE, E., LEROY, P., BORNARD, L., *Influence of the velocity field at the inlet of a Francis turbine draft tube on performance over an operating range*, IOP Conf. Ser.: Earth Environ. Sci. **15**, 032008, 2012.
6. SUSAN-RESIGA, R.F., MUNTEAN, S., AVELLAN, F., ANTON, I., *Mathematical modelling of swirling flow in hydraulic turbines for the full operating range*, Applied Mathematical Modelling, **35**, pp. 4759–73, 2011.
7. CIOCAN, T., SUSAN-RESIGA, R.F., MUNTEAN, S., A*nalysis of the swirling flow at GAMM Francis runner outlet for different values of the discharge*, Proc. of the XXXIIIrd Caius-Iacob Conference On Fluid Mechanics and Its Technical Applications, Bucharest, Romania, 2011, pp. 33–41.
8. SOTTAS, G., RYHMING, I.L., *3D – Computation of Incompressible Internal Flows*, Proc. of the GAMM Workshop, Notes Numerical Fluid Mechanics (NNFM), **39**, Braunschweig, Germany, 1993.
9. GUBIN, M.F., VOLSHANIK, V.V., KAZENNOV, V.V., *Investigations of curved draft tubes with long exit cones*, Hydrotechnical Construction, **8**, *10*, pp. 949–956, 1974.
10. INTERNATIONAL ELECTROTECHNICAL COMMISION, *Hydraulic Turbines. Storage Pumps and Pump-Turbines – Model Acceptance Tests*, International Standard IEC 60193, 2nd Ed., Geneva, Switzerland, 1999.
11. *** FLUENT INC., GAMBIT 2.4. User's Guide, Lebanon, New Hampshire, 2006.
12. *** FLUENT INC., FLUENT V6.3 User's Guide, Lebanon, New Hampshire, 2006.
13. MEAD, R., NELDER, J.A., *A simplex method function minimization*, Computer J., **7**, pp. 308–313, 1965.
14. PRESS, W.H., TEUKOLSKY, S.A., VETTERLING, W.T., FLANNERY, B.P., *Numerical Recipes in FORTRAN 77: The Art of Scientific Computing*, 2nd Ed., New York, Cambridge University Press, 1996.
15. ANTON, I., *Hydraulic turbines* (in Romanian), Facla Publishing House, Timisoara, 1979.
16. *** VISUAL NUMERICS INC., IMSL Fortran Library User's Guide. Mathematical Functions in Fortran, 2003.
17. SUSAN-RESIGA, R.F., CIOCAN, G.D., ANTON, I., AVELLAN, F., *Analysis of the swirling flow downstream a Francis turbine runner*, J. Fluids Eng., **128**, pp. 177–189, 2006.
18. TRIDON, S., BARRE, S., CIOCAN, G.D., SÉGOUFIN, C., LEROY, P., *Discharge imbalance mitigation in Francis turbine draft-tube bays*, J. Fluids Eng., **134,** 041102, pp. 8, 2012.
19. ZANGENEH, M., GOTO, A., HARADA, H., *On the role of three-dimensional inverse design methods in turbomachinery shape optimization*, Proc. of the Institution of Mechanical Engineers, Part C: Journal of Mechanical Engineering Science, **123**, *1*, pp. 27–42, 1999.

Received September 3, 2013